CEBAF-TH-90-02

Many-Body Correlation Effects on the Longitudinl Response in the Quasielastic (e, e′) Reaction

Patrick M. Boucher
Continuous Electron Beam Accelerator Facility
Newport News, VA 23606

J. W. Van Orden
Department of Physics, Old Dominion University
Norfolk, Virginia 23529-0116
and
Continuous Electron Beam Accelerator Facility
Newport News, VA 23606

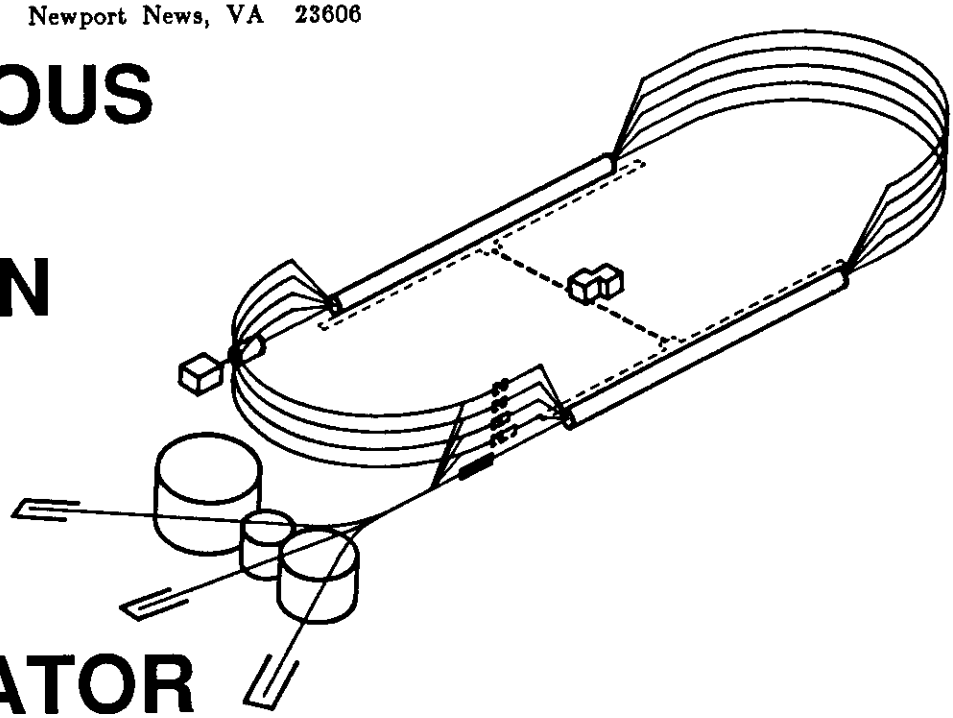

CONTINUOUS
ELECTRON
BEAM
ACCELERATOR
FACILITY

SURA Southeastern Universities Research Association

CEBAF
The Continuous Electron Beam Accelerator Facility

Newport News, Virginia

Copies available from:

Library
CEBAF
12000 Jefferson Avenue
Newport News
Virginia 23606

The Southeastern Universities Research Association (SURA) operates the Continuous Electron Beam Accelerator Facility for the United States Department of Energy under contract DE-AC05-84ER40150.

Many-Body Correlation Effects on the Longitudinal Response in the Quasielastic (e, e') Reaction

P. M. Boucher
Continuous Electron Beam Accelerator Facility
12000 Jefferson Ave, Newport News, Virginia 23606

J. W. Van Orden
Department of Physics, Old Dominion University, Norfolk, Virginia 23529-0116
and
Continuous Electron Beam Accelerator Facility
12000 Jefferson Ave, Newport News, Virginia 23606

A study is made of the influence of many-body corrections on the longitudinal response function for the inclusive quasielastic (e, e') reaction. This response function is well known to be suppressed, by about a factor of two, when compared with theoretical predictions based on the concept of single nucleon ejection. This is a characteristic of the data that persists through a wide range of different nuclei and suggests a violation of the Coulomb sum rule. It is here shown how an estimation of the effect of many-body correlations, including a consistent treatment of inelastic final state interactions, can be computed through a relationship to the nuclear optical model. The approximations are such that the Coulomb sum rule is guaranteed to remain satisfied providing the optical potential is hermitian analytic. Calculations of the longitudinal response are carried out within the Fermi Gas Model using phenomenological parameterizations of the nuclear optical potential. The reductions in both the peak strength and the total integrated response are significant, but not sufficient to explain the discrepancy between theory and experiment. The resulting distribution of strength is characterized by the energy-weighted sum rule which remains satisfied to the level of the approximations, about 5%.

I. INTRODUCTION

Several recent measurements[1-7] of the inclusive quasielastic (e, e') cross section have spurred considerable theoretical effort to understand them. The need for such attention is partly a consequence of the failure of traditional models to explain the separated longitudinal response. Even the simplest model of quasielastic scattering, the Fermi Gas Model in the impulse approximation, appeared to be extremely successful at explaining the unseparated data.[8] It thus proved surprising that this model fails by a factor of two to fit the longitudinal response functions alone. This suppression of the response is a systematic feature, observed in nuclei ranging from ^{12}C to ^{238}U, for several values of the momentum transfer between $q = 330\,\mathrm{MeV}$ and $q = 550\,\mathrm{MeV}$.

Even more importantly, the data suggest a violation[9-10] of a sum rule, first proposed by Heisenberg,[11] that demands the large q limit of the integrated response for point nucleons be Z, the total nuclear charge.[12] This apparent violation of the Coulomb sum rule has led to considerable speculation on the physical origin of the observed suppression. Several Random Phase Approximation (RPA) calculations have been carried out[13-14] and have provided a qualitative description of the longitudinal response at low momentum transfer. Above momentum transfers of 400 MeV, one-particle–one-hole (1p–1h) RPA effects tend to be very small,[15] and the need to include more complicated configurations through the second RPA (SRPA)[14-15] have been recognized. Thus, within the framework of nonrelativistic physics, the predominant explanation has been the effect of 2p-2h[13-15] and further many-body[17] correlations. It has also been suggested that the suppression may be due to modifications of the nucleon size within the medium (the "swollen nucleon" hypothesis),[18-37] quark clustering exchange effects,[26] and relativistic dynamical effects.[27-34]

While the influence of these more speculative mechanisms generally improve the agreement with experiment, they need to be considered cautiously to ensure that their appealing features are neither accidental nor pathological. Relativistic RPA (RRPA) calculations, for example, exhibit substantial suppressions that persist to large momentum transfer, but have relied on the σ–ω model[35] representation of the residual particle-hole interaction; it has recently been shown that this theory is not even qualitatively stable with respect to a loop expansion[36] and it is unclear to what extent the calculated suppression will endure a more realistic representation of the nucleon-nucleon interaction. In addition, renormalized RRPA calculations that use pointlike interactions are known to generate unphysical singularities at large momentum transfers.[37]

The assumption that a description of quasielastic scattering can be predicated on the concept of single nucleon ejection is difficult to justify. The momentum and energy

transfers involved in the experiments clearly allow scattering into many final state channels involving multiple nucleon ejection and a calculation of the inclusive response should involve contributions from all open final state channels. Many calculations have ignored the final state interactions because the total flux must be conserved; it is important to recognize, however, that the strength will be redistributed as a function of momentum and energy transfer due to differences in the coupling to the available phase space.

Currently, the most satisfactory way of including the effects of the final state interactions is the optical model Green function approach originally presented by Horikawa *et al.*:[38] a one-body approximation to quasielastic electron scattering can be constructed by exploiting the relationship between forward virtual Compton scattering and inclusive electron scattering. The result is a doorway model with the virtual photon being absorbed initially by a single nucleon that can couple to more complicated final channels through the final state interaction. The original motivation for this approximation was found in multiple scattering theory, but it was shown in the recent comprehensive study of final state interactions by Chinn *et al.*[33] how this approach can be derived using projection techniques.

Similar projection techniques have also been used[17] to account for the influence of many-body correlations on the longitudinal response by constructing an effective current operator to be used in the evaluation of the transition matrix element. This effective operator is related to the optical potential by using the projection techniques to account for the coupling to states more complicated than 1p–1h in an approximate way. Thus, it is possible to study the role of many-body correlations in a more consistent way by including the final state interactions through the optical model Green function approach. By exploiting the relationship to forward virtual Compton scattering, the projection techniques can be used to relate the exact many-body expression to a simplified version given in terms of the optical potential.

This is the formulation to which this paper is addressed. Because of the connection with the optical model, the final state interaction can be constrained by means of elastic nucleon-nucleus scattering; also, the substantial body of work on the derivation and properties of microscopic optical potentials can be exploited.[39–51] By introducing a reasonable set of approximations, the full many-body problem can be approximated by one in which the basis states are simply one-body states; this is at the expense of introducing effective current operators, but they are related to the energy dependent optical potential and are not unwieldy. Such a formulation allows the use of traditional models of quasielastic scattering to evaluate the full many-body longitudinal response. In particular, the simplicity of the Fermi Gas Model allows it to be used to study the role of many-body correlations in a comprehensive fashion.

The paper is organized in the following way. The general formalism is presented in the first part of the next section. The second part of that section is used to show in detail how the adopted set of valid approximations can be used to simplify the general expression so that the result is calculable. It is also proved that the Coulomb sum rule has not been compromised by the set of approximations. In Section III, details of the calculation within the Fermi Gas Model are presented. Some emphasis is placed on the way in which phenomenological optical potentials were used, especially at large momentum and energy transfers. Attention is drawn to the limitations of describing the nucleus as a Fermi gas in the appendix where the somewhat remarkable result, that the contributions from the single nucleon knockout channel vanish, is presented. Numerical results of the calculations are then discussed in Section IV. There is some sensitivity to the choice of optical potential parameterization seen. In addition, energy-weighted sum rules are used as a test of the consistency of the method. The final section is used to summarize the results and inferences that can be drawn from this study.

II. FORMALISM

A. Many-body corrections to the Longitudinal Response

Both the longitudinal and transverse response functions are defined in terms of the nuclear tensor, $W^{\mu\nu}(\mathbf{q},\omega)$, which involves the matrix elements of the virtual photon's interaction with the nuclear electromagnetic current,

$$\begin{aligned} R_L(\mathbf{q},\omega) &= W^{00}(\mathbf{q},\omega) \\ R_T(\mathbf{q},\omega) &= W^{11}(\mathbf{q},\omega) + W^{22}(\mathbf{q},\omega), \end{aligned} \tag{1}$$

with

$$W^{\mu\nu}(\mathbf{q},\omega) \equiv \overline{\sum_i} \sum_f \langle i|J^{\mu\dagger}(q)|f\rangle \langle f|J^{\nu}(q)|i\rangle \delta(E_f - E_i - \omega). \tag{2}$$

The $\overline{\sum}$ is used to denote an average of the A-body initial states $|i\rangle$ while $|f\rangle$ is a particular A-body final nuclear state. The electromagnetic current operator, J^{μ}, is a function of the four-momentum of the virtual photon $q = (\omega, \mathbf{q})$. Note that only the diagonal components of the response tensor are needed to define the inclusive response functions. These components can be written alternatively as imaginary parts of the virtual forward Compton amplitude, $T^{\mu\mu}$, *i.e.*, the contribution from the elastic scattering of virtual photons from the bound nucleus,

$$W^{\mu\mu} = -\frac{1}{\pi} \mathrm{Im}\, T^{\mu\mu} \tag{3}$$

where

$$T^{\mu\mu} \equiv \overline{\sum_i} \langle i|J^\mu(-q)G(E_i+\omega)J^\mu(q)|i\rangle \tag{4}$$

and $G(E)$ is the full A-body propagator.

At this stage, Eq. (4) retains all of the complexities of the many-body problem. From a practical standpoint it is useful to try to relate the exact expression to a simplified version given in terms of the optical model. This can be achieved by using the Feshbach operator projection method.[51] For simplicity, the derivation given below neglects complications associated with the antisymmetrization of the wave functions. It has been demonstrated, however, that a completely antisymmetrized theory can be constructed which retains the form of the simple unsymmetrized theory provided that an appropriate identification of the optical potential be made.[32,47-50] The form of the results obtained here is not, therefore, dependent upon this assumption and the generalization to a completely antisymmetric formalism is straightforward. Furthermore, it is assumed in the following derivation that the target nucleus has zero spin in order to simplify the labeling of states and to remove the average over initial states. This assumption can easily be eliminated and does not affect the form of the results obtained below.

In the Feshbach approach the A-body hamiltonian H is divided into two pieces: the first is an (A−1)-body interacting hamiltonian plus a kinetic energy term for the A^{th} nucleon, and is denoted by h; the other term is the residual interaction between the (A−1)-body system and the A^{th} nucleon and is denoted by V. That is,

$$H = h + V. \tag{5}$$

A projector onto an eigenstate of h can be defined as

$$P_\alpha = |\alpha\rangle\langle\alpha| \tag{6}$$

where

$$h|\alpha\rangle = E_\alpha|\alpha\rangle. \tag{7}$$

In this case a subset of the eigenfunctions of h corresponding to a finite set of excitations of the (A−1)-body system will be chosen. In interpreting the physical content of the approximations made below, it is useful to think of these states as the result of a hole being placed in the various filled shells of a closed shell nucleus. The projector onto the subspace spanned by these states is

$$P \equiv \sum_\alpha P_\alpha. \tag{8}$$

The orthogonal projector onto the remainder of the Hilbert space is, then,

$$Q \equiv 1 - P. \tag{9}$$

Note that by their definitions, only V and not h, connects the two subspaces:

$$PhQ = QhP = 0 \tag{10}$$

implies that

$$PHQ = PVQ \quad \text{and} \quad QHP = QVP. \tag{11}$$

Using these definitions, it is possible to project the A-body Schrödinger equation for the initial state $|i\rangle$ using

$$H(P+Q)|i\rangle = E_i|i\rangle. \tag{12}$$

Projection of Eq. (12) on the left with P and Q give the equations

$$(PHP + PVQ)\,|i\rangle = E_i P|i\rangle \tag{13}$$

and

$$(QVP + QHQ)\,|i\rangle = E_i Q|i\rangle. \tag{14}$$

Eq. (14) can be solved to give the Q-space projection of $|i\rangle$ in terms of its P-space projection,

$$Q|i\rangle = g_Q(E_i)QVP|i\rangle, \tag{15}$$

where

$$g_Q(E) \equiv \frac{1}{E - QHQ + i\eta} \tag{16}$$

describes propagation in the Q-space only. Using Eq. (15), the initial state can be expressed in terms of only its P-space projection,

$$|i\rangle = P|i\rangle + Q|i\rangle = (1 + g_Q(E_i)QVP)\,P|i\rangle. \tag{17}$$

Furthermore, Eqs. (13) and (14) can be solved to give

$$(PhP + PVP + PVQg_Q(E_i)QVP)\,P|i\rangle = E_i P|i\rangle. \tag{18}$$

which is an effective Schrödinger equation for $P|i\rangle$.

A similar, but slightly more complicated, approach can be used with the A-body propagator $G(E)$. The propagator can be written as

$$\begin{aligned} G(E) &= G_0(E) + G_0(E)VG(E) \\ &= G_0(E) + G(E)VG_0(E) \end{aligned} \tag{19}$$

with

$$G_0(E) \equiv \frac{1}{E - h + i\eta}. \tag{20}$$

Projection of Eq. (19) on the right and left by P and Q yields a set of coupled equations that can be solved to give

$$G(E) = (1 + g_Q(E)QVP)\, PG(E)P\, (1 + PVQg_Q(E)) + g_Q(E) \tag{21}$$

where

$$PG(E)P = PG_0(E)P + PG_0(E)P\, (PVP + PVQg_Q(E)QVP)\, PGP. \tag{22}$$

Using the expressions in Eqs. (17) and (21), the Compton amplitude defined in Eq. (4) can be written as

$$\begin{aligned} T^{\mu\mu} = \langle i| \Big(& PJ^{\mu}_{eff}(-q, E_i, E_i + \omega) PG(E_i + \omega) PJ^{\mu}_{eff}(q, E_i + \omega, E_i) P \\ & + (P + PVQg_Q(E_i)) J^{\mu}(-q) g_Q(E_i + \omega) J^{\mu}(q) (P + g_Q(E_i)QVP) \Big) |i\rangle \end{aligned} \tag{23}$$

where

$$PJ^{\mu}_{eff}(q, E', E)P \equiv (P + PVQg_Q(E'))J^{\mu}(q)(P + g_Q(E)QVP) \tag{24}$$

is an effective current operator in the P-space. Note that Eq. (23) consists of two terms. The first of these can be expressed entirely in terms of effective operators, states and propagators in the P-space, while the second involves intermediate propagation only in the Q-space and is not readily described in terms of effective P-space operators.

At this stage, Eqs. (18), (22), (23) and (24) should be viewed as matrix equations expressing the coupling of the various P_α subspaces. The expressions can be simplified considerably by assuming that each of three important pieces is diagonal in the P_α's: the effective current operator of Eq. (24); the second term of Eq. (23); and, finally, the effective potential that appears in both the effective Schrödinger equation, Eq.

(18), and the equation for the projected propagator, Eq. (21). The forward Compton amplitude then becomes

$$T^{\mu\mu} = \sum_{\alpha} \langle i | \Big(P_\alpha J^\mu_{eff}(-q, E_i, E_i+\omega) P_\alpha G(E_i+\omega) P_\alpha J^\mu_{eff}(q, E_i+\omega, E_i) P_\alpha + (P_\alpha + P_\alpha V Q g_Q(E_i)) J^\mu(-q) g_Q(E_i+\omega) J^\mu(q) (P_\alpha + g_Q(E_i) Q V P_\alpha) \Big) | i \rangle \quad (25)$$

The projection of the propagator $P_\alpha G(E) P_\alpha$ can be identified as the optical model Green function for the α channel, and satisfies the equation

$$P_\alpha G(E) P_\alpha \equiv G^\alpha_{opt}(E) = G^\alpha_0(E) + G^\alpha_0(E) V^\alpha_{opt}(E) G^\alpha_{opt}(E) \quad (26)$$

where

$$G^\alpha_0(E) \equiv P_\alpha G_0(E) P_\alpha \quad (27)$$

and the optical potential is defined as

$$V^\alpha_{opt}(E) \equiv P_\alpha V P_\alpha + P_\alpha V Q g_Q(E) Q V P_\alpha. \quad (28)$$

Note that the effective Schrödinger equation for the projected initial state, Eq. (18), then becomes

$$\Big(P_\alpha h P_\alpha + V^\alpha_{opt}(E_i) \Big) P_\alpha |i\rangle = E_i P_\alpha |i\rangle \quad (29)$$

where the optical potential is real below the Q-space threshold.

It is evident from Eq. (25) that a consistent treatment of the Compton amplitude requires a consistent construction of the optical potential, the effective current operators and the contributions represented by the second term in Eq. (25). While it may be possible to approximate the theoretical optical potential with some phenomenological interaction, the other elements in the calculation of Eq. (25) are not generally amenable to such treatment. However, the particular characteristics of the nonrelativistic charge operator allow for a reasonable set of approximations that permits the calculation of a realistic estimate of T^{00}, and thus R_L, using only information derived from phenomenological optical potentials. This involves corrections to previous calculations[32,33,38] based on the optical model that used the free charge operator in place of the effective one and neglected the contributions represented by the second term of Eq. (25). The approximations used below are similar to those introduced earlier in the context of the orthogonality problem in DWIA calculations of the $(e, e'p)$ reaction.[52] A more distantly related approach,[53] imposes conditions on the optical model propagator to obtain results which bear a superficial resemblence to those presented below.

The one-body charge density operator can be written as

$$\rho(q) \equiv J^0(q) = F_1(q^2) \sum_{i=1}^{A} \frac{1}{2}[1 + \tau_3^{(i)}] e^{i\mathbf{q}\cdot\mathbf{r}_i}$$
$$= \sum_{i=1}^{A} \rho_i(q), \tag{30}$$

where it has been assumed that the Dirac form factor of the neutron vanishes and that any exchange current contributions to the charge density operator are of higher order in v/c. The operator form of the continuity equation requires that

$$\mathbf{q} \cdot \mathbf{J}(q) = [H, \rho(q)]. \tag{31}$$

The current operator can be divided into a one-body contribution and a two-body meson exchange contribution. That is,

$$\mathbf{J}(q) = \mathbf{J}^{(1)}(q) + \mathbf{J}^{(2)}(q). \tag{32}$$

If the hamiltonian is written as

$$H \equiv T + \mathcal{V} \tag{33}$$

where T is the kinetic energy, and $\mathcal{V}$ is the two-body interaction potential, then the continuity equation for the free hamiltonian requires that

$$\mathbf{q} \cdot \mathbf{J}^{(1)}(q) = [T, \rho(q)]. \tag{34}$$

This implies that

$$\mathbf{q} \cdot \mathbf{J}^{(2)}(q) = [\mathcal{V}, \rho(q)] \cong 0 \tag{35}$$

owing to the fact that the exchange current contributions to the three-vector current are predominantly transverse. The only remaining contribution to $[H, \rho]$ comes from Eq. (34). The one-body current contains contributions from the convection and magnetization currents. Since the magnetization current is totally transverse, the only contribution which remains is that of the convection current. The commutator can thus be written as

$$[H, \rho] \cong [T, \rho] = \frac{1}{2m} \sum_i \rho_i(q)[\mathbf{q}^2 + 2\mathbf{q} \cdot \mathbf{p}_i]$$
$$\cong \frac{1}{2m} \sum_i \rho_i(q)\mathbf{q}^2$$
$$= E_q \rho(q) \tag{36}$$

where

$$E_q \equiv \frac{\mathbf{q}^2}{2m} \tag{37}$$

and because the angle-average of the scalar product $\mathbf{q}\cdot\mathbf{p}_i$ vanishes, terms involving it have been neglected. This is an approximation that can easily be checked numerically and was found to have a negligible affect on the calculations presented below.

The final, and most critical assumption, is that the charge density operator is diagonal in the P_α subspaces. That is

$$[\rho, P_\alpha] = 0 \tag{38}$$

which implies that

$$[\rho, P] = [\rho, Q] = 0. \tag{39}$$

These approximations can now be used to simplify the expression for T^{00} given in Eq. (25). Consider the relationship

$$\rho(q)\,[P_\alpha + g_Q(E_i)QVP_\alpha] \cong [P_\alpha + g_Q(E_i+E_q)QVP_\alpha]\,\rho^\alpha(q); \tag{40}$$

where

$$\rho^\alpha(\pm q) \equiv P_\alpha \rho(\pm q) P_\alpha. \tag{41}$$

and Eq. (40) follows from Eqs. (38) and (39), along with the results

$$\rho(q) g_Q(E_i) \cong g_Q(E_i+E_q)\rho(q) \tag{42}$$

and

$$[V, \rho(q)] \cong 0. \tag{43}$$

The first of these expressions, Eq. (42), is a consequence of Eqs. (16), (36), (38) and (39), while the second, Eq. (43), follows immediately from Eq. (35). It can similarly be shown that

$$[P_\alpha + P_\alpha VQ g_Q(E_i)]\,\rho(-q) = \rho^\alpha(-q)\,[P_\alpha + P_\alpha VQ g_Q(E_i+E_q)]\,. \tag{44}$$

Using Eq. (40)

$$\begin{aligned}
\rho^\alpha_{eff}(q, E_i+\omega, E_i) &= P_\alpha \rho_{eff}(q, E_i+\omega, E_i) P_\alpha \\
&= [P_\alpha + P_\alpha VQ g_Q(E_i+\omega)]\,\rho(q)\,[P_\alpha + g_Q(E_i)QVP_\alpha] \\
&\cong [P_\alpha + P_\alpha VQ g_Q(E_i+\omega)]\,[P_\alpha + g_Q(E_i+E_q)QVP_\alpha]\,\rho^\alpha(q) \\
&= [P_\alpha + P_\alpha VQ g_Q(E_i+\omega) g_Q(E_i+E_q)QVP_\alpha]\,\rho^\alpha(q).
\end{aligned} \tag{45}$$

Using

$$g_Q(E_i+\omega)g_Q(E_i+E_q) = -\frac{1}{\omega - E_q}\left[g_Q(E_i+\omega) - g_Q(E_i+E_q)\right] \tag{46}$$

and using the definition of the optical potential in Eq. (28), Eq. (45) can be written as

$$\rho^\alpha_{eff}(q, E_i+\omega, E_i) = \left[1 - \Gamma^\alpha(E_i+\omega, E_i+E_q)\right]\rho^\alpha(q) \tag{47}$$

where

$$\Gamma^\alpha(E,E') \equiv \frac{1}{E-E'}\left[V^\alpha_{opt}(E) - V^\alpha_{opt}(E')\right]. \tag{48}$$

Similarly, using Eq. (44)

$$\rho^\alpha_{eff}(-q, E_i, E_i+\omega) = \rho^\alpha(-q)\left[1 - \Gamma^\alpha(E_i+\omega, E_i+E_q)\right]. \tag{49}$$

Using Eqs. (40) and (44), the second term contributing to T^{00} in Eq. (25) can now be rewritten as

$$\begin{aligned}
&\left[P_\alpha + P_\alpha VQg_Q(E_i)\right]\rho(-q)g_Q(E_i+\omega)\rho(q)\left[P_\alpha + g_Q(E_i)QVP_\alpha\right] \\
&\quad\cong \rho^\alpha(-q)\left[P_\alpha + P_\alpha VQg_Q(E_i+E_q)\right]g_Q(E_i+\omega)\left[P_\alpha + g_Q(E_i+E_q)QVP_\alpha\right]\rho^\alpha(q) \\
&\quad= \rho^\alpha(-q)\left[P_\alpha + P_\alpha VQg_Q(E_i+E_q)g_Q(E_i+\omega)g_Q(E_i+E_q)QVP_\alpha\right]\rho^\alpha(q) \\
&\quad= \rho^\alpha(-q)\frac{1}{\omega - E_q}\left[\Gamma^\alpha(E_i+\omega, E_i+E_q) - V'^\alpha_{opt}(E_i+E_q)\right]\rho^\alpha(q)
\end{aligned} \tag{50}$$

where $V'^\alpha_{opt}(E)$ is the derivative of the optical potential with respect to energy and we have used the identity

$$\begin{aligned}
&g_Q(E_i+E_q)g_Q(E_i+\omega)g_Q(E_i+E_q) \\
&\qquad= \left(\frac{1}{\omega - E_q}\right)^2\left[g_Q(E_i+\omega) - g_Q(E_i+E_q)\right] - \frac{1}{\omega - E_q}g'_Q(E_i+E_q)
\end{aligned} \tag{51}$$

with $g'_Q(E)$ representing the derivative of the Q-space propagator with respect to the energy.

The forward virtual Compton amplitude T^{00} can be written as

$$\begin{aligned}
T^{00} = \sum_\alpha \langle i|\ \rho^\alpha(-q)\Big\{&\left[1 - \Gamma^\alpha(E_i+\omega, E_i+E_q)\right]G^\alpha_{opt}(E_i+\omega)\left[1 - \Gamma^\alpha(E_i+\omega, E_i+E_q)\right] \\
&+\frac{1}{\omega - E_q}\left[\Gamma^\alpha(E_i+\omega, E_i+E_q) - V'^\alpha_{opt}(E_i+E_q)\right]\Big\}\rho^\alpha(q)|i\rangle.
\end{aligned} \tag{52}$$

In order to establish a simple connection to the optical model in the above derivation, it was convenient to assume that all effective operators acting in the P space

were diagonal in the P_α subspaces and that the single-nucleon charge operator also had this property. As a result we have eliminated the dynamical coupling of P_α subspaces through either effective potentials or the charge operator. This implies that we have not included long range correlations of the RPA type; we therefore have not included collective excitations of the nucleus in the calculations of the forward virtual Compton amplitude T_{00} and thus in the longitudinal response R_L. Consequently, calculations based on this model will not properly reproduce the longitudinal response at low values of the three-momentum transfer where previous calculations have shown the collective degrees of freedom to be important. Equation (52) is most applicable to the determination of the effect of short range correlations on R_L at relatively large momentum transfers.

B. Coulomb Sum Rule

A nonrelativistic calculation of the type approximated above can be shown to satisfy the Coulomb sum rule[12]

$$\lim_{|\mathbf{q}|\to\infty} S_0(q) = \lim_{|\mathbf{q}|\to\infty} \int_{0+}^{\infty} d\omega \, \frac{R_L(\mathbf{q},\omega)}{F_1^2(q^2)} = Z. \tag{53}$$

A reasonable constraint on any approximation to such a theory should be the requirement that the Coulomb sum rule remain satisfied. It can be demonstrated that the expression Eq. (52) leads to a longitudinal response function that satisfies this constraint.

The first step in a proof of this result is to note that the optical potential as defined by Eq. (28) is hermitian analytic; that is

$$V_{opt}^{\alpha\dagger}(E) = V_{opt}^{\alpha}(E^*), \tag{54}$$

and the analytic structure of $V_{opt}^{\alpha}(E)$ can also be deduced from that of the propagator $g_Q(E)$ appearing in Eq. (28). Thus, the optical potential must satisfy a dispersion relation in the energy variable; since the imaginary part of the potential is asymptotically constant[42], a subtraction is necessary:[51,38,42]

$$\mathrm{Re}\, V_{opt}^{\alpha}(E) = \mathrm{Re}\, V_{opt}^{\alpha}(0) + \frac{E}{\pi}\mathcal{P}\int_{\varepsilon_0}^{\infty} \frac{dE'\ \mathrm{Im}\, V_{opt}^{\alpha}(E')}{E'(E'-E)}. \tag{55}$$

The dispersion integral begins at ε_0, the threshold energy for Q-space processes. This dispersion relation can be used to deduce the asymptotic behavior of $\mathrm{Re}\, V_{opt}^{\alpha}(E)$, which is evidently logarithmic. Given that the optical potential is changing at most logarithmically at large energies, it is clear that the large E_q behavior of Γ, as defined by Eq. (48) is dominated by the factor $(\omega - E_q)^{-1}$ and therefore

$$\lim_{E_q\to\infty}\Gamma^{\alpha}(E_i+\omega,E_i+E_q)=0. \tag{56}$$

Given this and the fact that $V'^{\alpha}_{opt}(E)$ must vary as E^{-1} for large E,

$$\lim_{E_q\to\infty}\frac{1}{\omega-E_q}\left[\Gamma^{\alpha}(E_i+\omega,E_i+E_q)-V'^{\alpha}_{opt}(E_i+E_q)\right]\Bigg\}=0. \tag{57}$$

The remaining contribution to the Coulomb sum rule is then the same as in previous optical model calculations of R_L as described in Refs. 32, 33 and 38. That is we have demonstrated that

$$\lim_{|\mathbf{q}|\to\infty}S_0=-\lim_{|\mathbf{q}|\to\infty}\frac{1}{\pi}\int_{0+}^{\infty}\frac{d\omega}{F_1^2(q^2)}\sum_{\alpha}\mathrm{Im}\langle i|\rho^{\alpha}(-q)G^{\alpha}_{opt}(E_i+\omega)\rho^{\alpha}(q)|i\rangle \tag{58}$$

In this expression the only contribution to the imaginary part of the matrix element is from the discontinuity in the optical potential. Since the optical potential is hermitian analytic, the optical model propagator can be expanded in a complete biorthogonal set of scattering wave functions.

$$G^{\alpha}_{opt}(E)=\sum_{\beta}\frac{|\psi^{\alpha(+)}_{\beta}(E)\rangle\langle\tilde{\psi}^{\alpha(+)}_{\beta}(E)|}{E-E_{\beta}+i\eta} \tag{59}$$

where

$$\left(P_{\alpha}hP_{\alpha}+V^{\alpha}_{opt}(E)\right)|\psi^{\alpha(+)}_{\beta}(E)\rangle=E_{\beta}|\psi^{\alpha(+)}_{\beta}(E)\rangle \tag{60}$$

and

$$\langle\tilde{\psi}^{\alpha(+)}_{\beta}(E)|\left(P_{\alpha}hP_{\alpha}+V^{\alpha}_{opt}(E)\right)=\langle\tilde{\psi}^{\alpha(+)}_{\beta}(E)|E_{\beta}. \tag{61}$$

Using this,

$$\lim_{|\mathbf{q}|\to\infty}S_0=\lim_{|\mathbf{q}|\to\infty}\int_{0+}^{\infty}\frac{d\omega}{F_1^2(q^2)}\sum_{\alpha}\langle i|\rho^{\alpha}(-q)\sum_{\beta}|\psi^{\alpha(+)}_{\beta}(E_i+\omega)\rangle$$
$$\times\delta(E_i+\omega-E_{\beta})\langle\tilde{\psi}^{\alpha(+)}_{\beta}(E_i+\omega)|\rho^{\alpha}(q)|i\rangle. \tag{62}$$

The factor $F_1^{-2}(q^2)$ cancels the form factors in the charge operator so that the only remaining dependence on ω is contained in the δ-function and can be removed trivially by the integral over ω. The completeness relation for the scattering wave functions

$$\sum_{\beta}|\psi^{\alpha(+)}_{\beta}(E)\rangle\langle\tilde{\psi}^{\alpha(+)}_{\beta}(E)|=1 \tag{63}$$

can then be used to give

$$\lim_{|\mathbf{q}|\to\infty}S_0=\sum_{\alpha}\langle i|P_{\alpha}\frac{1}{2}\left(1+\tau_3\right)P_{\alpha}|i\rangle\cong Z \tag{64}$$

provided that the set of P_{α} subspaces is chosen to approximately saturate the spectral strength. This demonstrates that the approximation represented by Eq. (52) will satisfy the Coulomb sum rule.

III. CALCULATIONS

The effect of the many-body correlations on the longitudinal response has been evaluated within the context of the Fermi Gas Model, described in detail in many standard texts.[54] The use of such a simple model is advantageous, at this stage, since it can readily be adopted for application to different nuclei and offers an opportunity to test extensively various features of the formalism, such as the saturation of the Coulomb sum rule and the degree to which other sum rules are satisfied. In this section, the methods used to implement the formalism presented in the preceeding section are described in detail. The numerical results and discussion of them are reserved for the following section. The wave functions used in the Fermi Gas Model are plane waves. This is because the model is characterized by the assumption that the nuclear system is large with periodic boundary conditions imposed over some normalization volume.

The final approximation made in evaluating the result presented in Eq. (52) is that the optical potential for each channel is the same,

$$V^{\alpha}_{opt}(E) \equiv V_{opt}(E), \tag{65}$$

with V_{opt} being the specific one-body optical potential associated with the initial target nucleus. As a result of this assumption, Eq. (65), the factor Γ defined in Eq. (48) is also unchanged between different α channels,

$$\Gamma^{\alpha}(E_i+\omega, E_i+E_q) \equiv \Gamma(E_i+\omega, E_i+E_q) = \frac{1}{\omega - E_q}\left[V_{opt}(E_i+\omega) - V_{opt}(E_i+E_q)\right]. \tag{66}$$

In the numerical calculations, spin-independent phenomenologically determined potentials are used. Since the system is infinite, the optical potential should have no radial dependence; for the calculations, the central value of the potential was adopted.

Inserting complete sets of states into Eq. (52) and introducing the wave functions explicitly, allows the expression for the Compton amplitude to be written in terms of a simple integral over occupied momentum states. The first term in Eq. (52) is closely related to the Compton amplitude in the absence of correlations,

$$T^{00}_{(\alpha)} = \frac{3Z}{4\pi k_F^3} F_1^2(q^2) \int d\mathbf{k}\, \theta(k_F - |\mathbf{k}|)[1-\Gamma(E_i+\omega, E_i+E_q)] G_{opt}(\mathbf{k}+\mathbf{q}, \mathbf{k}+\mathbf{q}, E_i+\omega) \times [1-\Gamma(E_i+\omega, E_i+E_q)]\theta(|\mathbf{k}+\mathbf{q}| - k_F), \tag{67}$$

Note that the usual expression for the longitudinal response function in the Fermi Gas Model can be recovered by setting the optical potential to zero; this amounts to replacing the optical model Green function with the unperturbed Green function,

G_0, and setting $\Gamma = 0$. The second term in the Compton amplitude is related to a density-density correlation function and is calculated in the same way. Within the context of the Fermi Gas Model for a spin-independent optical potential, it takes the form,

$$T^{00}_{(b)} = \frac{3Z}{4\pi k_F^3} F_1^2(q^2) \int d\mathbf{k}\, \theta(k_F - |\mathbf{k}|) \times \frac{1}{\omega - E_q} \left[\Gamma(E_i + \omega, E_i + E_q) - V'_{opt}(E_i + E_q)\right] \theta(|\mathbf{k} + \mathbf{q}| - k_F). \quad (68)$$

The evaluation of the longitudinal response thus becomes a matter of performing the numerical integration of the integrals appearing in Eqs. (67) and (68):

$$R_L(\mathbf{q}, \omega) = -\frac{1}{\pi} \mathrm{Im}(T^{00}_{(a)} + T^{00}_{(b)}). \quad (69)$$

It is always judicious to exercise caution when considering a model that treats the nucleus as an infinite system, since there are obvious limitations inherent in such an approach. In the appendix, it is demonstrated that the contribution of the single nucleon knockout channel to the response vanishes in the Fermi Gas Model. This seems initially surprising but is merely a reflection of the impossibility of ejecting a single nucleon from an infinite system with an absorptive potential.

Several comments are needed to make clear the way in which the phenomenological optical potentials were handled. Parameterizations of the optical potential rely on data determined from proton-nucleus and neutron-nucleus elastic scattering experiments. Consequently, the parameterizations are valid only over a limited range of energies for which the data have been determined reliably. It is desirable to have a potential that can be used at larger energies for two reasons: first, experiments at the largest momentum transfer values have provided data at reasonably large excitation energies, often beyond the highest energy at which a parameterization is expected to be reliable; second, it is important to understand the large momentum transfer saturation of the Coulomb sum rule value in the presence of many-body correlation effects.

A distinction need now be drawn between the "generalized optical potential" introduced by Feshbach[51] and the phenomenological optical potential that is deduced from experimental data. The nonlocal generalized optical potential must satisfy the dispersion relation, Eq. (55), but there is no guarantee that the phenomenological potential will do so because of the assumption of locality. The energy dependence of the empirical potential arises from both nonlocal effects and the dispersive nature of nuclear matter. At low energies, the construction of an optical potential depends on an energy average because the presence of resonances is important.[51,42] At sufficiently

high energies, the distinction between the two potentials disappears. The application of the dispersion relation is, thus, justified only if the dispersion integral is dominated by the high energy contribution. The analysis by Passatore[42] was carried out, in part, to show that this is the case and that the dispersion relation can be used reliably to extend the optical potential to larger energies. At the same time, a potential was constructed semi-phenomenologically by fitting only the imaginary part of the optical potential with data and calculating the real part directly from the dispersion relation. Thus, this potential was adopted for the calculations of the many-body longitudinal response function. As a potential constructed specifically to have the correct analytic structure, it is particularly useful in studying the large momentum transfer behavior of the response and the saturation to the Coulomb sum rule value.

In addition, a more realistic low energy potential constructed by fitting independently the real and imaginary parts to experimental data, was considered. For this purpose, the more recent parameterization of Schwandt *et al.*[41] was adopted. This potential was fit with proton scattering data up to 180 MeV. The real part of the potential was logarithmically parameterized and includes a small constant symmetry energy term; the imaginary part was cubically parameterized. The real part thus behaves at larger energies in a manner consistent with expectations from the dispersion relation, while the imaginary part does not. Simply extending the real part to arbitrarily large energy and invoking the dispersion relation demands that the asymptotic value of the imaginary part be π times the coefficient of the logarithm. In the case of the Schwandt potential this asymptotic value is, then, -54 MeV, a value consistent with the Passatore and other optical potential analyses. So, in using the Schwandt potential, the real part was simply extended, but the imaginary part was artificially bounded to be > -54 MeV.

In the figures presented below, a comparison is made between the present calculation and a previous calculation[17] to which allusions were made in the introduction. It follows from using the projection scheme directly on the transition matrix element:

$$R_L^{(o)}(\mathbf{q},\omega) = \sum_f |\langle f|\rho(q)|i\rangle|^2 \delta(E_i + \omega - E_f) \tag{70}$$

with

$$\langle f|\rho(q)|i\rangle \cong \sum_\alpha \langle f|P_\alpha \rho(q)[1 - \Gamma^\alpha(E_i+\omega, E_i+E_q)]P_\alpha|i\rangle. \tag{71}$$

Evidently the calculation of this quantity both ignores the contributions of the final state interaction between the ejected nucleon and the residual nucleus, and does not treat as consistently the various pieces that enter into the expression of the full response. That the present treatment is to be preferred, because all of the pieces of

the calculation are treated equally, will be particularly evident from the discussion of sum rules presented below. For comparison, the calculations of $R_L^{(o)}$ have been carried out using the Schwandt parameterization of the optical potential.

To compare with the available experimental data, the fit to the nucleon form factor produced by Hohler *et al.*[55] was used. Substantial differences in the predicted response functions can be produced with alternative choices of the form factor, but the use of the Hohler fit provides a fair evaluation of the nonrelativistic response.

IV. RESULTS

The evaluation of Eq. (69) for the longitudinal response, R_L, has been carried out with a Fermi momentum value of $k_F = 268\,\mathrm{MeV}$. While data are available for several nuclei, the Fermi Gas Model calculations are largely insensitive to differences between nuclei. The assumption of an infinite system eliminates the sensitivity to any shell structure particularities. The Passatore parameterization of the optical potential makes no distinction between nuclei and while the Schwandt parameterization contains a symmetry energy term, it is small. There are no significant differences in the resulting response functions of, for example, ^{40}Ca, ^{48}Ca and (except for a scaling of 26/20) ^{56}Fe. It is thus prudent to focus on the calculations for ^{40}Ca which typify the Fermi Gas Model calculations.

The excitation energy dependence of the response functions is displayed for a range of momentum transfer values from 410 MeV to 550 MeV in Fig. (1). The results of the full many-body calculations are shown by the solid and short-dashed lines, corresponding to the use of the Schwandt and Passatore parameterizations of the optical potential respectively. These are to be contrasted with the free Fermi Gas Model calculations shown by the dotted lines and the $R_L^{(o)}$ approximation of Eq. (70) shown by the long dashed line. The effect of the many-body correlations is seen to redistribute the strength. A significant contribution to the response functions is seen at large energies. It is apparent that the results using the two parameterizations are similar despite the significantly greater tendency for strength to be pushed up in energy when the Schwandt potential is used. This is primarily a consequence of the behavior of the imaginary part of the Schwandt potential; it is considerably deeper in the energy range associated with the experimental results. As the momentum transfer increases, one can see that the difference between the free and many-body curves decreases: at 410 MeV, the peak height is reduced by about 35%, while at 550 MeV it is reduced by about 25%.

The role of the different pieces involved in the total many-body response function is exhibited by Fig. (2), where only the Schwandt parameterization is studied. Again the free Fermi Gas Model and $R_L^{(o)}$ results are shown by the dotted and long dashed lines

for comparison. The results show systematically the effect of including different pieces: the short dashed lines show only the role of the final state interactions determined from the calculation when $\Gamma \equiv 0$. The tendency for the strength to be redistributed to higher energies is partly a consequence of the imaginary part of the optical potential. There is also a well-known tendency for the Fermi Gas Model response function to spread as a result of the reactive real part of the potential. The second term in Eq. (69) has very little influence; the contribution to the response from it is too small to be seen in the figures. The solid line shows the final result, with all of the pieces of the calculation included. The peak of the response function is only modestly decreased by the final state interactions, and the predominant supression of the response is seen to result from the role of the many-body correlations. The peak height supression due to the final state interactions is typically about 5 to 10%. The difference between the results of the preliminary calculation of $R_L^{(o)}$ and the present, fully-consistent calculation is also significant.

The final figure, Fig. (3), is used to show the resulting sum rule values for the full calculations as functions of the momentum transfer. In part (a), the integrated response in the absence of form factors, Eq. (53), has been normalized to Z. The saturation of the sum rule with increasing q is seen to be retained. In part (b), the response function has been integrated with the form factor to allow a comparison with experiment. As anticipated, the influence of the many-body effects is greatest at low momentum transfer values and slowly die as q is increased. A careful examination of the figures will reveal some features that may at first appear peculiar. First, there is an apparent cusp in the Schwandt potential results; this is an artifact of the arbitrary floor imposed on its imaginary part. Notice that this occurs only near the greatest momentum transfer values tested experimentally and that the general trend is still manifest. Second, the results using the Passatore potential appear to be converging to a CSR value slightly less than Z; this is because the imaginary part of the Passatore potential more slowly reaches its asymptotic value, achieving it only well above 1 GeV.

In part (c) of Fig. (3) a further test of the consistency of the technique is carried out. The energy-weighted sum rule is a construction that depends on the completeness of the set of excited states reached by the density operator acting on the ground state, subject to the approximations made in the evaluation of the response:

$$S_{+1}(q) \equiv \int_{0+}^{\infty} d\omega\, \omega \frac{R_L(q,\omega)}{F_1^2(q^2)} = \frac{q^2}{2m} Z. \tag{72}$$

The energy-weighted sum rule has been normalized by $(q^2/2m)Z$ for display in the figure. The present calculations are much more satisfactory than those which follow from Eq. (70) since they can only describe the suppression of the response at lower energy without clearly showing how it must be redistributed and reappear at larger

energy. The deviations of the present calculations from the sum rule value are less than 5% and are greater when the Schwandt potential is used. This should be viewed together with the findings of Horikawa et al.[38] which indicated that sum rule violations up to 10% could be expected when using phenomenological potentials. That the Passatore potential was constructed on the basis of its theoretical analytic structure is the reason why it does so much better. Again, a careful examination of the figure will reveal a subtlety. The energy-weighted sum rule value of the results using the Passatore potential dips slightly at low momentum transfer values. This can be attributed to the fact that the potential was constructed with the dispersion relation and high energy behavior in mind. Consequently, the imaginary part of the Passatore potential does not vanish at $\omega = 0$ and a small fraction of the low energy strength is lost.

That the sum rules remain satisfied by this calculation means that the effect of the many-body correlations is to redistribute the energy-weighted strength in a way that reduces the total non-energy-weighted integrated response. It has been suggested by Noble[56] that such a mechanism is inconsistent with existing experimental data. His argument is based on the relationship between the Coulomb and energy-weighted sum rules, defined in Eqs. (53) and (72). Since the effect of correlations is to push the strength to higher energies it is frequently argued that reductions in the quasielastic region should be accompanied by a corresponding increase at energies larger than have been measured. Noble has used the fact that this mechanism will affect the ratio S_1/S_0 to determine from experiment the effective energy at which missing strength should reappear:

$$\omega_{eff} = \frac{1}{\chi}\left[(1+\chi)\left(\frac{S_1}{S_0}\right)_{th} - \left(\frac{S_1}{S_0}\right)_{exp}\right], \tag{73}$$

where χ is the fraction of the non-energy-weighted strength that is missing. Simple calculations then reveal that ω_{eff} lies in the experimental region. Data were available for Noble to perform his calculations at momentum transfer values $\leq 410\,\mathrm{MeV}$; using recent data at larger values of the momentum transfer, the effective energy is larger (relative to $q^2/2m$) but still within the experimental region. This observation has been partly confirmed by these calculations which show the redistributed strength still to lie mainly within the experimental region although there are some long high-energy tails that would be difficult to measure. It should be emphasized, however, that the reductions in the integrated response are significant and that the discrepancy from experiment is reduced by the inclusion of correlations. Furthermore, it is now well known that the overall shape of the data is not as narrowly peaked as suggested by simple theories and that a simple scaling of the theoretical curves is not sufficient;

the correlation effects appear necessary to broaden the response functions so that the shape is more in line with experiment.

A very recent study[57] has concerned itself with the inverse energy-weighted moment,

$$S_{-1}(q) \equiv \int d\omega \, \frac{R_L(q,\omega)}{\omega F_1^2(q^2)}, \tag{74}$$

which is proportional to the nuclear polarizability. The authors of that analysis have performed a constrained Thomas-Fermi calculation and found the calculated polarizabilities to be in good agreement with the values determined from the experimental response functions. They have, thus, cautioned that mechanisms invoked to explain the quenching of the longitudinal response and CSR should not severely affect the polarizability. In the case of the noninteracting Fermi Gas Model, the polarizability can be computed analytically and is consistently greater than the experimental results by factors of 1.5 to 2.0. The effect of the present calculations on the polarizability is to decrease it at low momentum transfer and have it increase steadily with q, reaching the free value near 500 MeV and continuing to increase beyond. The agreement with experiment is not significantly better or worse than achieved with the free Fermi Gas Model. In any case, the technique presented here is not particularly well-suited to reproduce the low energy part of the response to which the polarizability is most sensitive. That the agreement with the inverse energy-weighted moment is not significantly improved by this method of including many-body correlations should not be viewed as a serious flaw.

V. SUMMARY AND CONCLUSIONS

The effects of many-body correlations on the longitudinal response in the quasielastic (e,e') reaction have been studied. Using standard projection techniques, an approximation to the longitudinal response function, including many-body correlations and final state interactions in a consistent way, has been derived. The technique relates full A-body states, through an optical potential, to the projection of those states on a subspace spanned by a finite set of excitations of an (A$-$1)-body system. The principal result of the paper is summarized by Eq. (52).

A numerical study of the contributions from different effects has been carried out within the Fermi Gas Model, using phenomenological parameterizations of the optical potential. The role of the correlations is significant. The integrated longitudinal response is suppressed by about 30% at a momentum transfer of 330 MeV. The suppression decreases steadily with q, reaching about 15% at 550 MeV, the largest momentum transfer studied experimentally. This trend is in line with both physical intuition and the general formalism: it has been shown that the effect of the correla-

tions must vanish asymptotically if the optical potential is hermitian analytic. This is borne out by the numerical calculations, which heal above 1 GeV.

The effect of the correlations can be characterized in terms of the energy-weighted sum rule, which demands that the energy-weighted integral of the response, at a fixed momentum transfer value, not vary as a consequence of their inclusion. This sum rule has been tested numerically and is satisfied to the level of the approximations made, about 5%. To simultaneously reduce the non-energy-weighted strength and still satisfy this sum rule, the strength is redistributed to higher excitation; substantial contributions appear in long high-energy tails that would be difficult to measure.

The choice of optical potential is important. Two parameterizations have been compared, one determined entirely from phenomenology (Schwandt[41]) and the other (Passatore[42]) determined semi-phenomenologically with a dispersion relation. While the qualitative features of the results using each of them are similar, their particular characteristics manifest themselves in the resulting response functions. For example, the Schwandt potential was fit only up to 180 MeV; the asymptotic behavior can be deduced from the dispersion relation, but there is an influential region in the extension above 180 MeV that has a deep imaginary part. This tends to push more strength to high energy than the other parameterization. By contrast, since the Passatore potential was fit only to the imaginary part, it is not as reliable in the energy region accessible experimentally.

In conclusion, it should be emphasized again that many-body correlation effects make substantial reductions in the longitudinal response, but not sufficiently to account for the discrepancy with experiment. A natural extension of this work would be to perform a microscopic finite nucleus calculation. This would overcome any ambiguity associated with the properties of infinite nuclear matter. The fact that the present results still overestimate the response suggests that other mechanisms are also important and that the full explanation of the problem is likely a combination of effects.

ACKNOWLEDGEMENTS

This work was supported by the U. S. Department of Energy and by the Natural Sciences and Engineering Research Council of Canada.

APPENDIX

It is worthwhile emphasizing that the Fermi Gas Model is inherently limited as a model of the nucleus, and that one must be cautious in interpreting results of calculations using it. An example of this is proved in this appendix: the Fermi

Gas Model predicts that the contribution to the response from the single nucleon knockout channel is zero. This is surprising, especially since the free Fermi Gas Model calculations were predicated on single nucleon knockout. To see that this is the case, consider operator discontinuities, defined to be the difference between operators and their hermitian adjoints, $\Delta A \equiv A - A^\dagger$,

$$R_L = \frac{i}{2\pi} \sum_\alpha \langle i | \Delta \widehat{T}^{00}_\alpha | i \rangle. \tag{75}$$

In this expression, $\widehat{T}^{00}_\alpha$ is the operator sandwiched between states in Eq. (52). After noting that the one-body current operator is hermitian, the term that need be considered is the discontinuity of the optical model Green function, deduced from the second resolvent identity, Eq. (19),

$$\Delta G_{opt} = (1 + V_{opt} G_{opt})^\dagger \Delta G_0 (1 + V_{opt} G_{opt}) + G^\dagger_{opt} \Delta V_{opt} G_{opt}. \tag{76}$$

It is the first term in this expression that contributes to the single nucleon knockout channel. The second term, as well as other contributions to $\Delta \widehat{T}^{00}_\alpha$, involve the discontinuity of the optical potential. This is just twice the imaginary part of the optical potential and contains information about all channels other than the single nucleon knockout channel. The discontinuity of the free propagator is simple,

$$\Delta G_0 = \frac{1}{E_i + \omega - h + i\eta} - \frac{1}{E_i + \omega - h - i\eta} = -2\pi i \delta(E_i + \omega - h). \tag{77}$$

The operator $(1 + V_{opt} G_{opt})$ is the Möller operator and distorts plane waves. In the Fermi Gas Model, however, the states must be plane waves and only the wave number can be shifted. Writing the Möller operator as

$$1 + V_{opt} G_{opt} = \frac{G_0^{-1}}{G_0^{-1} - V_{opt}} = \frac{E_i + \omega - h}{E_i + \omega - h - V_{opt}} \tag{78}$$

makes this more clear. In the Fermi Gas Model, the only contribution to the single nucleon knockout channel thus comes from terms proportional to

$$\left[\frac{E_i + \omega - E_{\mathbf{k}}}{E_i + \omega - E_{\mathbf{k}} - V_{opt}} \right]^\dagger \delta(E_i + \omega - E_{\mathbf{k}}) \left[\frac{E_i + \omega - E_{\mathbf{k}}}{E_i + \omega - E_{\mathbf{k}} - V_{opt}} \right] = 0, \tag{79}$$

and so the *total* contribution to the response comes from other channels. This is a reflection of the impossibility of ejecting a single nucleon from an infinite system with an absorptive potential.

[1]C. C. Blatchley *et al.*, Phys. Rev. C **34**, 1243 (1986).

[2]M. Deady *et al.*, Phys. Rev. C **33**, 1897 (1986); **28**, 631 (1983).

[3]B. Frois, Nucl. Phys. **A434**, 57 (1985).

[4]A. Hotta *et al.*, Phys. Rev. C **30**, 87 (1984).

[5]Z. E. Meziani *et al.*, Phys. Rev. Lett **52**, 2130 (1984); **54**, 1233 (1985); Nucl. Phys. **A46**, 113c (1985).

[6]P. Barreau *et al.*, Nucl. Phys. **A402**, 515 (1983); **A358**, 287c (1981).

[7]R. Altemus *et al.*, Phys. Rev. Lett. **44**, 965 (1980).

[8]E. J. Moniz, Phys. Rev. **184**, 1154 (1969); E. J. Moniz, I. Sick, R. R. Whitney, J. Ficenec, R. D. Kephart and W. P. Trower, Phys. Rev. Lett. **26**, 445 (1971); R. R. Whitney, I. Sick, J. Ficenec, R. D. Kephart and W. P. Trower, Phys. Rev. C **9**, 2230 (1974); J. W. Van Orden, Ph.D. thesis, Stanford University (1978).

[9]G. Do Dang, M. L'Huillier, N. Van Giai and J. W. Van Orden, Phys. Rev. C **35**, 1637 (1987).

[10]G. Orlandini and M. Traini, Phys. Rev. C **31**, 280 (1985).

[11]W. Heisenberg, Z. Phys. **32**, 737 (1931).

[12]T. deForest and J. D. Walecka, Ann. Phys. (N. Y.) **15**, 1 (1966); W. Donnelly and J. D. Walecka, Ann. Rev. Nucl. Sci. **25**, 729 (1975).

[13]U. Stroth, R. W. Hasse and P. Schuck, Nucl. Phys. **A462**, 45 (1987); Phys. Lett. **171B**, 339 (1986); W. M. Alberico, A. Molinari, A. DePace, M. Ericson and M. B. Johnson, Phys. Rev. C **34**, 977 (1986); F. A. Brieva and A. Dellafiore, *ibid.* **36**, 899 (1987); C. Có and S. Krewald, Nucl. Phys. **A433**, 392 (1985); M. Cavinato *et al.*, *ibid.* **A423**, 376 (1984).

[14]G. Có, K. F. Quader, R. D. Smith and J. Wambach, Nucl. Phys. **A485**, 61 (1988); R. D. Smith and J. Wambach, Phys. Rev. C **38**, 100 (1988); C. Drozdz, G. Có, J. Wambach and J. Speth, Phys. Lett. **185B**, 287 (1987); G. Có, K. Quader and J. Wambach, Proceedings of the Second Workshop on Problems of Theoretical Nuclear Physics, Cortona, Italy (1987) [University of Illinois Report Ill-(NU)-87-58, (1987)].

[15]S. Fantoni and V. R. Pandharipanda, Nucl. Phys. **A473**, 234 (1987).

[16]J. Jaenicke, P. Schuck, U. Stroth and R. W. Hasse, J. Phys. C **2**, 71 (1987);

J. Jaenicke, P. Schuck and R. W. Hasse, Phys. Lett. **214B**, 1 (1988).

[17]P. M. Boucher, B. Castel, Y. Okuhara and H. Sagawa, Ann. Phys. (N. Y.) **196**, 150 (1989); H. Sagawa, P. M. Boucher, B. Castel and Y. Okuhara, Phys. Lett. **219B**, 10 (1989).

[18]J. V. Noble, Phys. Rev. Lett. **46**, 412 (1981); Phys. Lett **178B**, 285 (1986).

[19]H. Kurasawa and T. Suzuki, Phys. Lett. **208B**, 160 (1988); **211**, 500(E) (1988); L. S. Celenza, A. Rosenthal and C. M. Shakin, *ibid.*, **53**, 892 (1984); Phys. Rev. C **31**, 232 (1985).

[20]I. Sick, Phys. Lett. **157B**, 13 (1985).

[21]L. S. Celenza, A. Harindranath and C. M. Shakin, Phys. Rev. C **33**, 1012 (1986).

[22]P. J. Mulders, Nucl. Phys. **A459**, 525 (1986).

[23]G. van der Steenhoven *et al.*, Phys. Rev. Lett. **57**, 182 (1986).

[24]M. Traini, Phys. Lett. **171B**, 266 (1986).

[25]T. D. Cohen, J. W. Van Orden and A. Picklesimer, Phys. Rev. Lett. **59**, 1267 (1987)

[26]P. J. Mulders, Phys. Rev. Lett. **54**, 2560 (1985); T. deForest and P. J. Mulders, Phys. Rev. D **35**, 2849 (1987); P. J. Mulders and A. E. L. Dieperink, Nucl. Phys. **A483**, 461 (1988); P. J. Mulders, Phys. Rep. **159**, 83 (1990).

[27]G. Do Dang and Nguyen Van Giai, Phys. Rev. C **30**, 731 (1984)

[28]R. Rosenfelder, Ann. Phys. (N.Y.) **128**, 188 (1980).

[29]H. Kurasawa and T. Suzuki, Phys. Lett. **173B**, 377 (1986); **A454**, 527 (1986); S. Nishizaki, H. Kurasawa and Toshio Suzuki, Phys. Lett. **171B**, 1 (1986); S. Nishizaki, T. Maruyama, H. Kurasawa and T. Suzuki, Nucl. Phys. **A485**, 515 (1988)

[30]C. J. Horowitz, Indiana University Report No. IU/NTC 88-4; in *Proceedings of the Workshop on Relativistic Nuclear Many-Body Physics, Columbus, 1988*, edited by B. C. Clark, R. J. Perry and J. P. Vary (World Scientific, Singapore, 1989).

[31]K. Wehrberger and F. Beck, Phys. Rev. C **35**, 298 (1987); C **37**, 1148 (1988).

[32]C. R. Chinn, A. Picklesimer and J. W. Van Orden, Phys. Rev. C **40**, 1159 (1989).

[33]C. R. Chinn, A. Picklesimer and J. W. Van Orden, Phys. Rev. C **40**, 790 (1989).

[34]X. Ji, Phys. Rev. C **39**, 1668 (1989); Phys. Lett. **219B**, 143 (1989).

[35]J. D. Walecka, Ann. Phys. (N. Y.) **83**, 491 (1974); B. D. Serot and J. D. Walecka, Adv. Nucl. Phys. **16**, 1 (1986).

[36]R. J. Furnstahl, R. J. Perry and B. D. Serot, Phys. Rev. C **40**, 321 (1989).

[37]T. D. Cohen, M. K. Banerjee and C. Y. Ren, Phys. Rev. C **36**, 1653 (1987).

[38]Y. Horikawa, F. Lenz and Nimai C. Mukhopadhyay, Phys. Rev. C **22**, 1680 (1980).

[39]K. Nakayama and W. G. Love, Phys. Rev. C **38**, 51 (1988).

[40]M. M. Giannini, G. Ricco and A. Zucchiatti, Ann. Phys. (N. Y.) **124**, 208 (1980)

[41]P. Schwandt *et al.*, Phys. Rev. C **26**, 55 (1982).

[42]G. Passatore, Nucl. Phys. **A95**, 694 (1967).

[43]A. Picklesimer, P. C. Tandy, R. M. Thaler and D. H. Wolfe, Phys. Rev. C **29**, 1582 (1984); **30**, 1861 (1984).

[44]M. V. Hynes, A. Picklesimer, P. C. Tandy and R. M. Thaler, Phys. Lett. **52**, 978 (1984); Phys. Rev. C **31**, 1438 (1985).

[45]J. A. McNeil, J. R. Shepard and S. J. Wallace, Phys. Rev. Lett. **50**, 1429 (1983); J. R. Shepard, J. A. McNeil and S. J. Wallace, *ibid.* **50**, 1443 (1983); B. C. Clark, S. Hama, R. L. Mercer, L. Ray and B. D. Serot, *ibid.* **50**, 1644 (1983).

[46]E. D. Cooper *et al.*, Phys. Rev. C **36**, 2170 (1987); E. D. Cooper, B. C. Clark, S. Hama and R. L. Mercer, Phys. Lett. **206B**, 588 (1988); bf 220, 658(e) (1989).

[47]K. L. Kowalski and A. Picklesimer, Phys. Rev. Lett. **46**, 228 (1981); Nucl. Phys. **A369**, 336 (1981).

[48]R. Goldflam and K. L. Kowalski, Phys. Rev. Lett. **44**, 1044 (1980); Phys. Rev. C **22**, 949 (1980).

[49]A. Picklesimer, Phys. Rev. C **24**, 1400 (1981).

[50]E. R. Siciliano and R. M. Thaler, Phys. Rev. C **16**, 1322 (1977); A. Picklesimer and R. M. Thaler, *ibid.* **23**, 42 (1981).

[51]H. Feshbach, Ann. Phys. (N. Y.) **5**, 357 (1958); **19**, 287 (1962); Ann. Rev. Nucl. Sci. **8**, 49 (1958).

[52]S. Boffi, F. Cannata, F. Capuzzi, G. Giusti and F. D. Pacati, Nucl. Phys. **A379**,

509 (1982).

[53]F. Capuzzi, C. Giusti and F. D. Pacati, University of Pavia Report No. FNT/T-90/03 (1990).

[54]A. Bohr and B. R. Mottelson, **Nuclear Structure, Vol. I**, W. A. Benjamin, New York, pp. 139ff (1969).

[55]G. Hohler *et al.*, Nucl. Phys. **B114**, 505 (1976).

[56]J. V. Noble, Phys. Rev. C **27**, 423 (1983).

[57]C. García-Recio, H. Krivine, Nguyen Van Giai and J. Navarro, Nucl. Phys. **A507**, 385 (1990).

FIG. 1. The longitudinal response function, R_L, for ^{40}Ca at momentum transfer values $q = 410$ MeV, 450 MeV, 500 MeV and 550 MeV is displayed in units of MeV^{-1}. The dotted (·····) curves represent the free Fermi gas calculation results and the long dashed (— — —) curves display the effects of the many-body correlations in the previous approximation of Eq. (70), $R_L^{(o)}$. The short dashed (- - - - -) curves show the effect of many-body correlations when the Passatore (dispersion relation) potential[42] is used and the solid (————) curves correspond to the same calculations using the Schwandt potential[41]. The experimental data are taken from Ref.[5] and have units MeV^{-1}.

FIG. 2. A comparison of the role of different effects in the many-body calculation using the Schwandt potential[41] is shown for the typical case of ^{40}Ca. The dotted (·····) curves correspond to the free Fermi Gas Model results; the short dashed (- - - - -) curves show the effect of final state interactions ($\Gamma \equiv 0$); the long dashed (— — —) curves show many-body correlation effects in the previous approximation of Eq. (70), $R_L^{(o)}$, and the solid (————) curves show the results of the full calculation. The effects of the density-density correlation term, $T_{(b)}^{00}$ are too small to be shown at this scale. The experimental data are taken from Ref.[5] and have units MeV^{-1}.

FIG. 3. The saturation of the Coulomb sum rule (CSR) and the energy-weighted sum rule are examined for the case of ^{40}Ca. In part (a), the form factor has been divided out and the integrated response function has been normalized by $Z(= 20)$. In part (b), the form factor has been retained for comparison with the experimental data. In the last part, part (c), the energy-weighted sum rule (EWSR) has been tested by evaluating the integral of the energy-weighted response without the form factor and normalized to the sum rule value, $q^2/2m$. The data are taken from Ref.[5]; in the case of parts (a) and (c), the deForest prescription has been used to remove form factor effects from the data.[32]

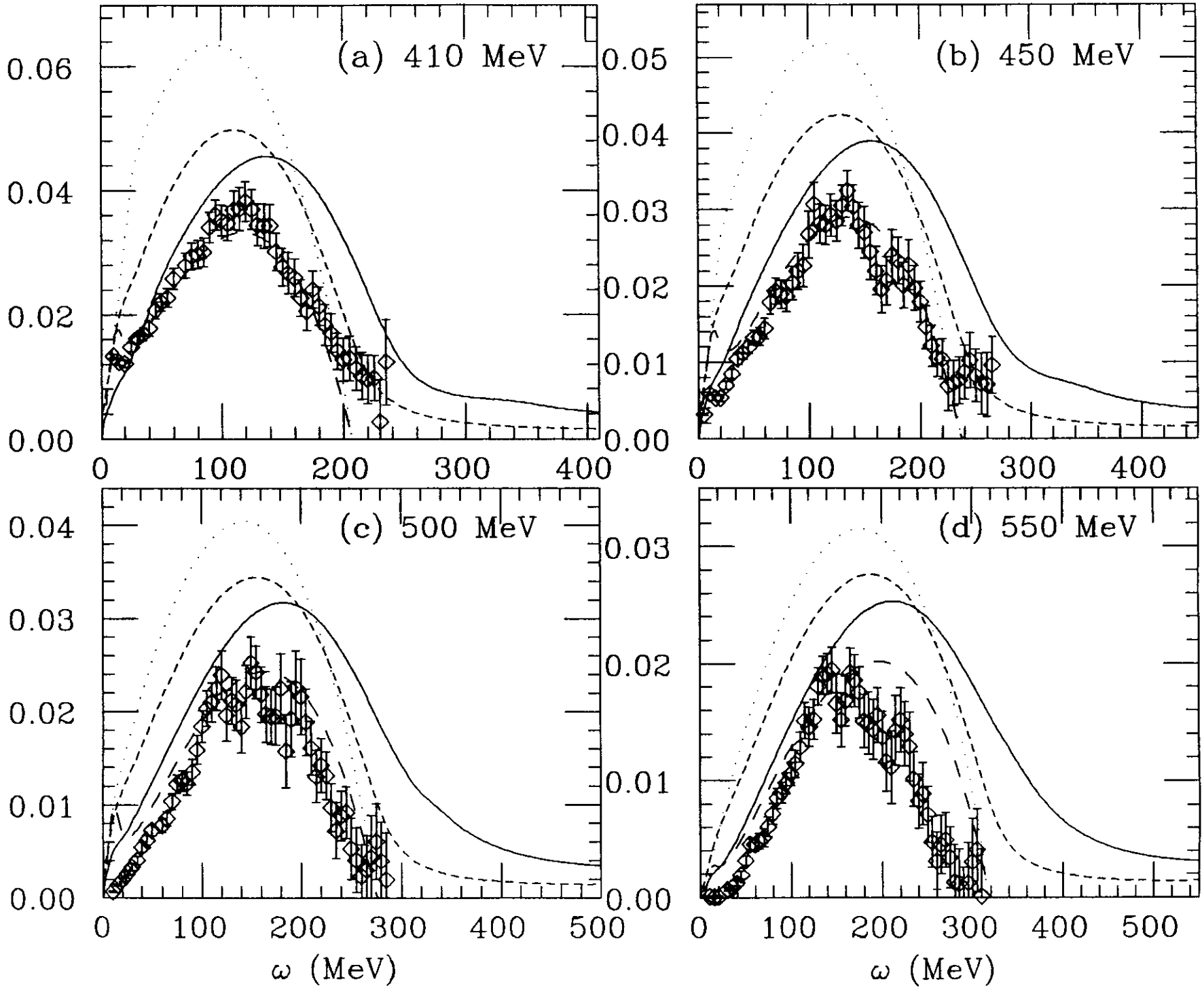
(a) 410 MeV
(b) 450 MeV
(c) 500 MeV
(d) 550 MeV
0.06
0.04
0.02
0.00
0.05
0.04
0.03
0.02
0.01
0.00
0.04
0.03
0.02
0.01
0.00
0.03
0.02
0.01
0.00
0
100
200
300
400
500
ω (MeV)

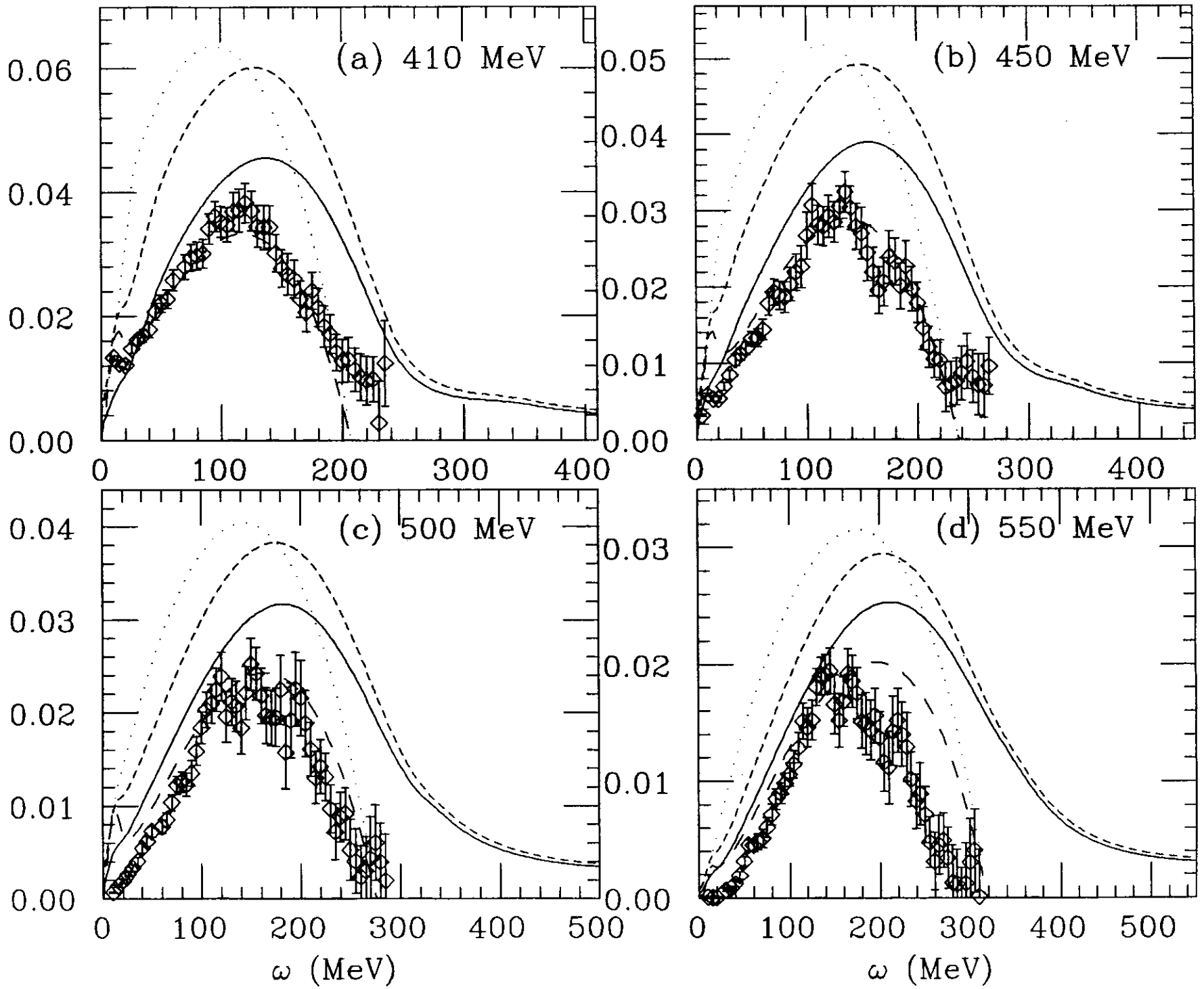
(a) 410 MeV
(b) 450 MeV
(c) 500 MeV
(d) 550 MeV
0.06
0.04
0.02
0.00
0.05
0.04
0.03
0.02
0.01
0.00
0.04
0.03
0.02
0.01
0.00
0.03
0.02
0.01
0.00
0
100
200
300
400
500
ω (MeV)

Fig. 3

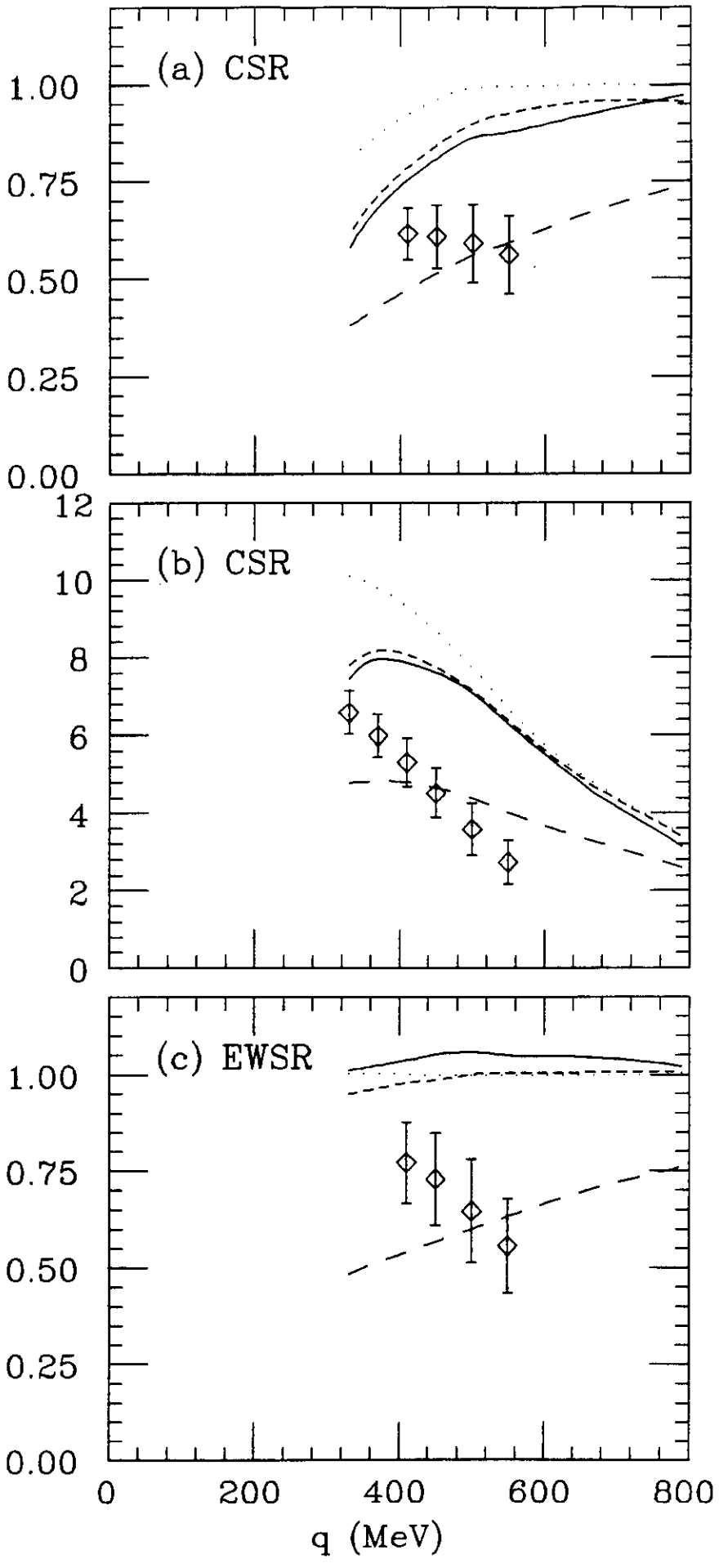
(a) CSR
1.00
0.75
0.50
0.25
0.00
12
(b) CSR
10
8
6
4
2
0
(c) EWSR
1.00
0.75
0.50
0.25
0.00
0
200
400
600
800
q (MeV)

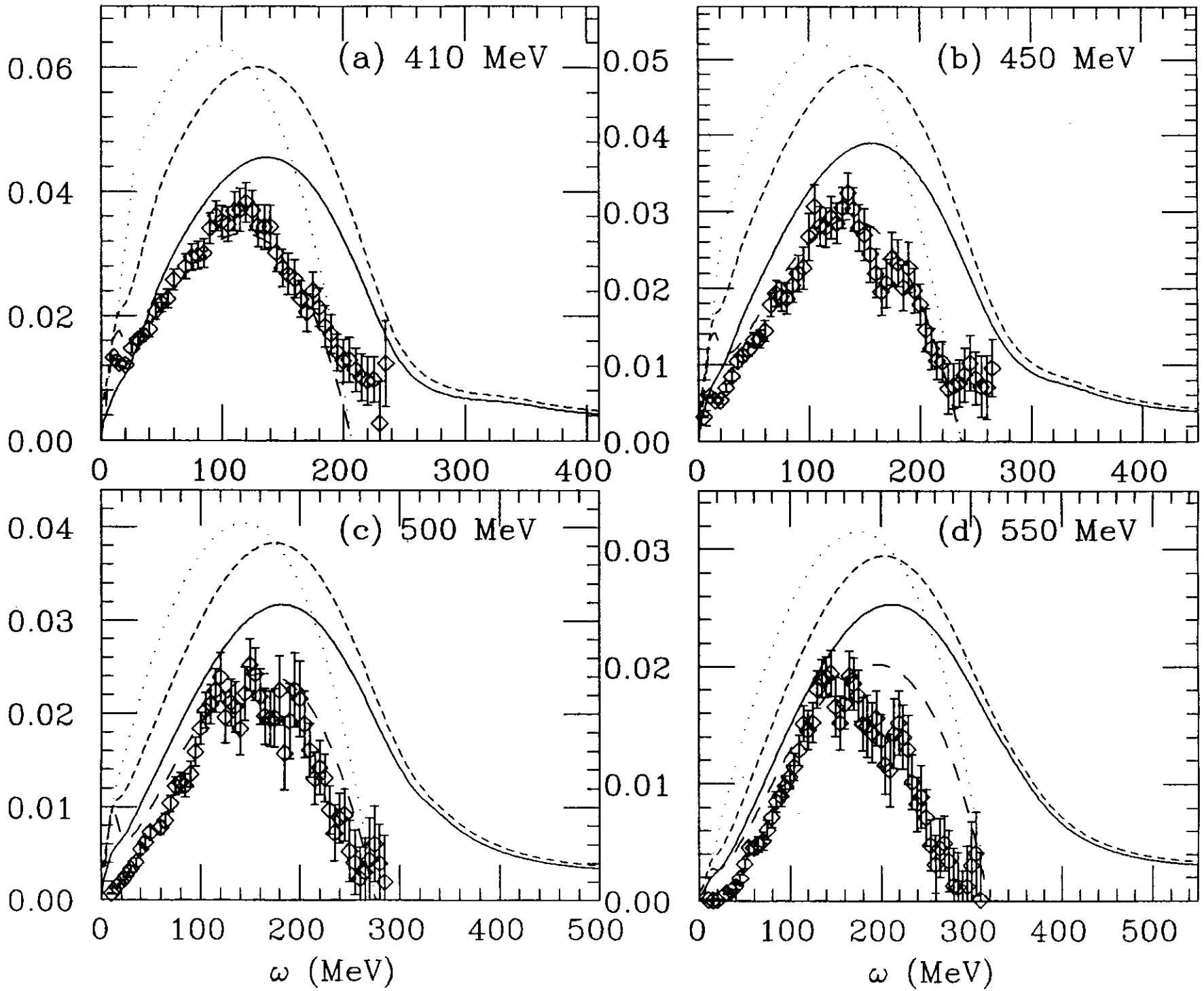
(a) 410 MeV
(b) 450 MeV
(c) 500 MeV
(d) 550 MeV
0.06
0.04
0.02
0.00
0.05
0.04
0.03
0.02
0.01
0.00
0.04
0.03
0.02
0.01
0.00
0.03
0.02
0.01
0.00
0
100
200
300
400
500
ω (MeV)